THE AMERICAN SOCIETY OF MECHANICAL ENGINEERS
Three Park Avenue, New York, N.Y. 10016-5990

99-GT-153

ON THE DEVELOPMENT AND APPLICATION OF THE FRAP® (FAST-RESPONSE AERODYNAMIC PROBE) SYSTEM IN TURBOMACHINES PART 2: FLOW, SURGE AND STALL IN A CENTRIFUGAL COMPRESSOR

Christian Roduner, Peter Kupferschmied, Pascal Köppel, George Gyarmathy

Turbomachinery Laboratory
Institute of Energy Technology
ETH - Swiss Federal Institute of Technology
8092 Zurich, Switzerland
http://www.lsm.iet.ethz.ch/lsm/

ABSTRACT

The present paper, Part 2 of a trilogy, is primarily focussed on demonstrating the capabilities of a FRAP® system configuration based on the simplest type of fast-response probe. A single cylindrical probe equipped with a single pressure sensor is used to measure absolute pressure and both velocity components in an essentially two-dimensional flow field. The probe is used in the *pseudo-3-sensor* mode (see Part 1). It is demonstrated that such a 1-sensor probe is able to measure high-frequency rotor-governed systematic fluctuations (like blade-to-blade phenomena) alone or in combination with flow-governed low-frequency fluctuations as rotating stall (RS) and mild surge (MS). However 3-sensor probes would be needed to measure stochastic (turbulence-related) or other aperiodic velocity transients.

The data shown refer to the impeller exit and the vaned diffuser of a single-stage high-subsonic centrifugal compressor. Wall-to-wall probe traverses were performed at the impeller exit and different positions along the vaned diffuser for different running conditions. The centrifugal compressor was operated under stable as well as under unstable (pulsating or stalled) running conditions. The turbomachinery oriented interpretation of these unsteady flow data is a second focus of the paper. A refined analysis of the time-resolved data will be done in Part 3 where different spatial/temporal averaging methods are compared.

Two different averaging methods were used for the data evaluation. Impeller based ensemble averaging for blade-to-blade systematic fluctuations (with constant period length at a constant shaft speed) and flow-based class averaging for the relatively slow MS and RS with slightly variable period length.

Due to the ability of fast-response probes to simultaneously measure velocity components as well as total and static pressure, interesting insights can be obtained into impeller and diffuser channel flow structures as well as into the time behavior of large-domain phenomena as RS and MS.

NOMENCLATURE

A	area
b	diffuser width (axial)
C	specific speed
c	velocity
L	length of diffuser vane
M	Mach number
Mu	impeller tip speed Mach number
$\dot{m}$	mass flow
p	pressure
R	gas constant
r	radius
r*	radius ratio
t	diffuser vane thickness, time
u	circumferential speed
$\dot{V}$	flow rate
z	axial coordinate
α	flow angle (diffuser coordinates)
$\alpha_{B\ vane}$	diffuser vane leading edge blade angle
ϑ	circumferential diffuser position
φ	specific flow rate $\left(\varphi = \frac{\dot{V}_1}{D_2^2 \cdot u_2}\right)$

Subscripts

1	impeller inlet
2	impeller outlet
3	diffuser outlet
A	measurement position in the diffuser
B	diffuser vane leading edge
E	measurement position in the diffuser
e	excitation
I	stage inlet
K	curvature
r	radial

Presented at the International Gas Turbine & Aeroengine Congress & Exhibition
Indianapolis, Indiana — June 7–June 10, 1999
This paper has been accepted for publication in the Transactions of the ASME
Discussion of it will be accepted at ASME Headquarters until September 30, 1999

RS	rotating stall
MS	mild surge
s	static
t	total

INTRODUCTION

The highly complex and fluctuating flow field at the exit of centrifugal compressor impellers and within diffuser vane channels (e.g. TRAUPEL 1988, DEAN and SENOO 1960, ECKARDT 1975, INOUE and CUMPSTY 1984) have been variously investigated by hot-wire techniques (DEAN and SENOO 1960, BAMMERT and RAUTENBERG 1974, INOUE and CUMPSTY 1984) and by optical methods (RUNSTADLER and DOLAN 1975, ECKARDT 1976, KRAIN 1981, HATHAWAY, CHRISS, WOOD and STRAZISAR 1993). Wall pressure transducers have been included in many rigs (BAMMERT 1974, DEAN and YOUNG 1977, KÄMMER and RAUTENBERG 1982) and were crucial in detecting mild surge and rotating stall. Pressure probes equipped with fast-response transducers have been successfully used in axial-flow compressors and turbines (e. g. NG and EPSTEIN 1985, WALBAUM and RIESS 1998) but were rarely used in centrifugal compessors (ECKARDT 1975).

All of the above methods have strengths and weaknesses. Multiple hot-wire probes give 3D comprehensive unsteady velocity information at low and moderate Mach numbers. Laser techniques are non-intrusive and suited to any Mach number. None of the above are capable of yielding static or total pressure data. Fast-response pressure probes are an intrusive technique measuring pressures and the velocity vector. Miniaturization of the probe head is required in order to minimize the intrusion effects (see Part 1of the present trilogy).

The present paper is aimed at demonstrating the use of ETH's fast-response aerodynamic probe system (FRAP®) to measure the high-frequency, high-amplitude flow fluctuations in the very inhomogeneous and turbulent flow field downstream of the impeller in a high speed subsonic centrifugal compressor. The measurements comprised steady-state as well as unstable operating conditions in the centrifugal compressor stage of the Turbomachinery Laboratory of the ETH (HUNZIKER 1993, RIBI 1996).

An overview of compressor instabilities in general is given in GREITZER (1981). In the compressor presented herein different instabilities occur along a speedline and their sequence depends on the shaft speed level. They are described in HUNZIKER and GYARMATHY (1993) and RIBI and GYARMATHY (1993). Two types of instabilities are treated here. Mild surge is a system (stage and piping) instability occurring at low flow rate and positive speedline gradients. Rotating stall is an in-stage instability and could be made stationary for the stage configuration presented herein only at a low shaft speed. The probe measurements allow one to investigate the temporal and spatial evolution of large-domain surge and stall processes.

Fast-response measurements deliver large amounts of data that have to be statistically treated, condensed, and critically analysed. A refined treatment of the data will be made in Part 3 of the present trilogy.

TEST STAND

The experiments described were performed on a closed loop test rig using air, see Fig. 1. The centrifugal compressor is an unshrouded industrial stage and is driven by a 440 kW DC-motor coupled to a two stage gear box. The flow rate is controlled by a throttle and is measured by a standard orifice ("DIN 1952" 1982). A flow straightener mounted in the suction pipe ensures axial flow at the stage inlet.

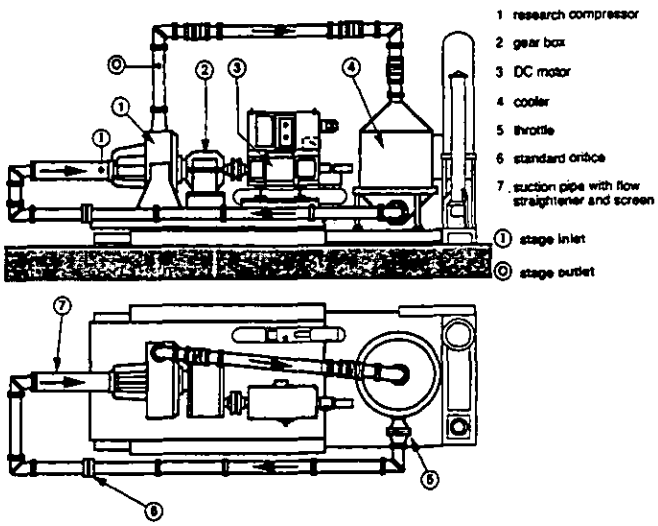

Fig. 1: General view of the centrifugal compressor test rig

During measurements the inlet temperature was held at 24°C and the pressure in the suction pipe was set to 960 mbar.

Fig. 2 shows the impeller and diffuser with the casing shroud removed. The configuration seen is used for all measurements described in this paper.

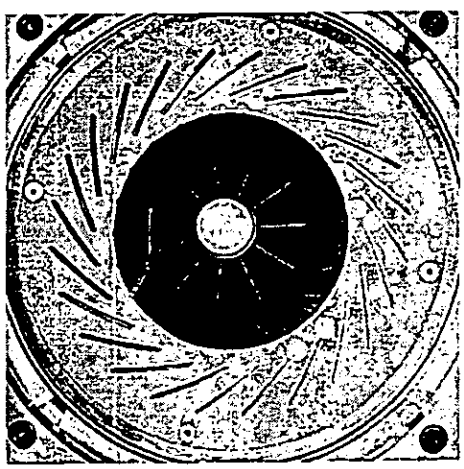

Fig. 2: View of unshrouded impeller and diffuser (configuration: 24 vanes, blade angle 25°)

The main data of the impeller were:

impeller tip diameter ($2r_2$)	280 mm
full/splitter blades	11/11 (total 22)
exit blade angle	30° back lean
exit width b	16.8 mm

The diffuser configuration used for the measurements consists of two parallel walls and 24 prismatic, circular-arc vanes. The leading edge blade angle $\alpha_{B\ vane}$ was set to 25°. Additional geometric data of the diffuser are given in Fig. 3.

The radial diffuser is followed by a large-diameter toroidal

collecting chamber (Fig. 4, grey parts) providing a virtually uniform circumferential pressure distribution at the impeller outlet under all throughflow conditions (HUNZIKER 1993).

The overall performance of the compressor was determined by conventional wall pressure taps and temperature probes in the suction pipe and in the outlet tube. A large number of conventional wall pressure taps are located in the front and the rear diffuser walls. These wall-tap pressure data are measured with a 256-channel pressure data acquisition system. All data were collected by a μVAX computer.

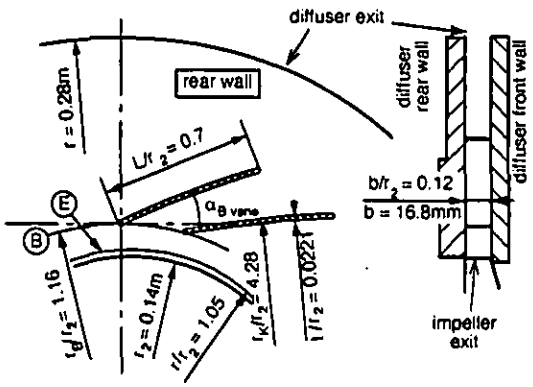

Fig. 3: Geometry of the vaned diffuser

MEASUREMENT SYSTEM

The probe measurement system used for this campaign is described in detail in Part 1 of this contribution.

Earlier investigations (RODUNER, KÖPPEL, KUPFERSCHMIED and GYARMATHY 1998) have demonstrated the capabilities of the system to measure absolute flow values in centrifugal compressors like the present one with high accuracy. As a typical example, mass flow calculated from a 1-sensor fast-response probe traverse at "best point" (Mu = 0.75) compared to the standard orifice measurements showed a difference of only 0.2%.

EXPERIMENTAL SET-UP

The probe actuator can be mounted (Fig. 4) on the front wall of the diffuser at eleven different positions I to XI (Fig. 5). Measurements taken at Pos. I, VI, VII and IX (in Fig. 5 indicated with black) are presented and discussed in the following.

The height b of the diffuser channel is 16.8 mm. Three-component LDV measurements performed in this test rig (STAHLECKER and GYARMATHY 1998) have shown that the axial component of the velocity vector is at least one order of magnitude smaller than the other two components. In the present paper the diffuser flow will be regarded as being 2-dimensional.

In order to avoid introducing a 3D disturbance into an otherwise 2D flow field, the free-ending tip of the probe was eliminated by using a cylindrical co-axial device shown in Fig. 6. A cylinder having the same diameter like the probe is mounted in the rear wall of the diffuser and kept in constant touch with the probe tip by a low-force pneumatic piston. Thus all probe-end effects are eliminated. This arrangement has the great advantage that no mechanical stresses are applied to the probe sensors.

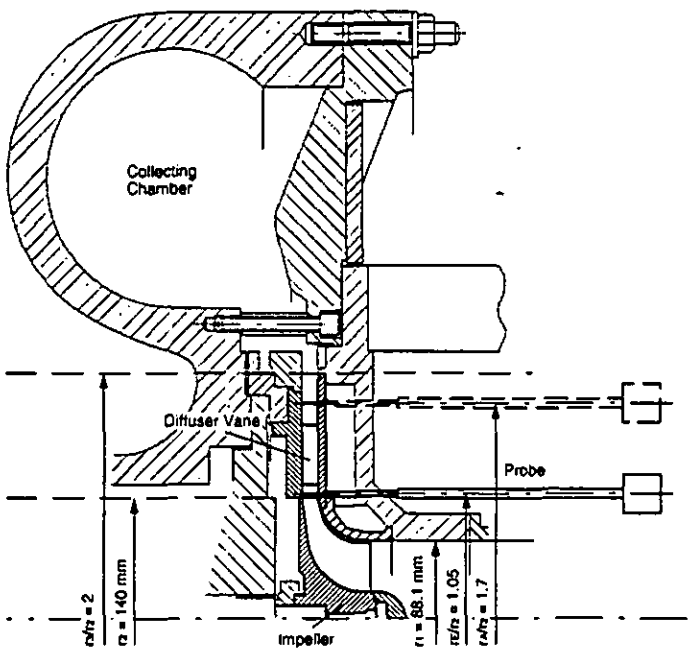

Fig. 4: Cross-sectional view of the centrifugal compressor with probe locations

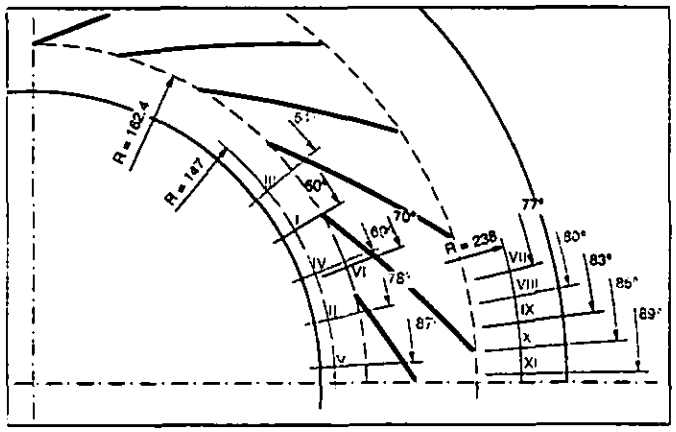

Fig. 5: Top view of the diffuser with probe positions I to XI (grey numbers: positions not discussed here)

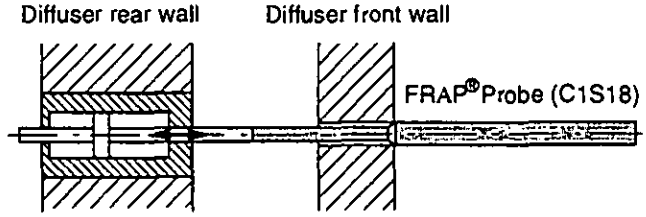

Fig. 6: Sketch of the auxiliary cylinder used to eliminate probe-tip effects

RUNNING CONDITIONS AND PERFORMANCE MAP

Measurements taken at four different running conditions of the test rig are presented. Two of them are located in the stable range of the performance map (Fig. 7) and two can be found in the unstable range. The four running conditions are indicated with flags in the performance map (Fig. 7). Measurements taken during stable running conditions are "best point" (BP) and "near surge" (NS). BP is the running condition at a given speed line with the highest efficiency. NS is the operating point with the lowest flow rate for stable operation at the given shaft speed. "Mild surge" (MS) and "rotating stall" (RS) are located in the unstable range of the performance map. During MS systematic pressure fluctuations occur in the entire system resulting in a periodic variation of the flow rate and the pressure rise coefficient of the compressor. A generic description of this phenomenon is given by GREITZER (1981). For the present compressor MS has been investigated in detail by RIBI (1997). RS is an instability of the stage. It is measured and described by many authors (e.g. JANSEN 1964, KÄMMER and RAUTENBERG 1982). A zone with blocked flow is travelling around in circumferential direction with approximately 28% of the shaft speed. In the present compressor a single cell full span rotating stall was found to exist.

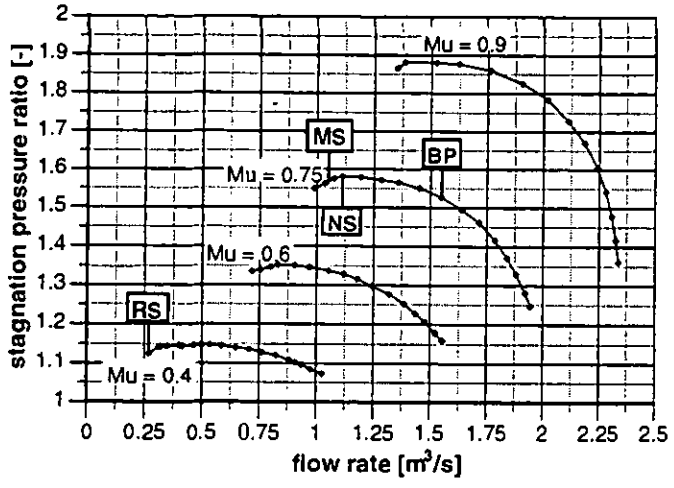

Fig. 7: Performance map of the standard configuration of the centrifugal compressor

Op. pt.	abbre-viation	$\dot{V}$ [m³/s]	$\dot{m}$ [kg/s]	φ [-]	rpm
best point	BP	1.553	1.757	0.0768	17720
near surge	NS	1.118	1.264	0.0553	17720
mild surge	MS	1.052	1.192	0.0521	17720
rotating stall	RS	0.268	0.306	0.025	9442

Tab. 1: Overview of the operating points used

For the BP, NS and MS points the compressor was operated at 17720 rpm, i. e. in the high subsonic regime (corresponds to impeller tip Mach number of Mu = 0.75). Long-time stable RS can only be observed at 9440 rpm (i. e., Mu = 0.4) in subsonic flow regime. In Tab. 1 an overview of the corresponding compressor data is given for all measured operating points.

MEASUREMENT PROCEDURES AND DATA EVALUATION

All measurements presented herein were performed with a 1-sensor fast-response probe (C1S18). In terms of the *systematic* fluctuations, this probe provides 2D velocity, total and static pressure in steady or periodically unsteady flows. Two alternative measurement procedures were applied. In practical situations the proper procedure has to be selected according to the predominant flow effects to be investigated.

Measurement procedure for stable running conditions of the test rig with the fast-response 1-sensor probe (C1S18)

In stable running conditions of the compressor the unsteady effects are due to periodic non-uniformities caused by the passage of blades and the stochastic fluctuations caused by turbulence.

The probe was used at every traverse position in a *pseudo-3-sensor* mode: the fluctuating flow was measured time-resolved under three angular positions of the probe shaft. The middle of the three angle positions was set to the known time-averaged flow direction. For the other two angle positions the probe was rotated (in yaw) by 43° to the left and the right, respectively. In each yaw position the sensor signal was measured and stored for a large number (over 240) of impeller revolutions, starting from a once per revolution trigger signal delivered by an optical trigger on the impeller shaft. By ensemble averaging over the revolutions all stochastic fluctuations were cancelled and the deterministic ones were obtained over a period equalling one impeller revolution. (This procedure also cancels periodic fluctuations having frequencies alien to the shaft speed if such frequencies are present in the flow.) The ensemble averaged data chains obtained for the three yaw positions simulate the periodic signals that would be delivered by a 3-sensor probe having sensors in the same yaw positions (KUPFERSCHMIED 1998).

The aerodynamic calibration-based data evaluation (see Part I) of the pressure fluctuations thus obtained provides the time-resolved flow values at a given traverse position. By taking these data traverse-point by traverse-point the circumferential systematic flow fluctuations over the diffuser channel height can be plotted. Such plots are shown in Fig. 10 to Fig. 15.

In order to achieve a statistically significant number of events the sampling rate of the data acquisition system was set to 200 kHz. With a rotation frequency of 295 Hz (17720 rpm) and a data collection time of 0.82 sec at each yaw position, 242 revolutions are measured and averaged. With an rotation frequency of about 295 Hz and a sampling rate of 200 kHz a resolution of 678 data points per revolution is achieved. This results in angular resolution of about 0.5°. Thus each ensemble to be averaged contained 200'000 * 0.82 / 678 = 242 events which were considered to be statistically sufficient.

Measurement procedure for unstable running conditions of the test rig with the fast-response 1-sensor probe (C1S18)

In unstable running conditions a third class of flow fluctuations is superposed on blade passing and turbulence effects. This is typically of much lower frequency and may be caused by mild surge (MS) in the piping system or by rotating stall (RS) in the compressor stage.

Importantly, the period length of MS or RS is subjected to irregular variations. Ensemble averaging with respect to such irregular phenomena requires a subdivision of each period into a constant number of time steps (called classes) rather than keeping the time steps constant. This sort of ensemble averaging will be termed "class averaging".

Measurement procedure during MS. Flow with MS was investigated in two ways. Once with the well known method where the data are ensemble averaged with a once per revolution trigger. In this case the impeller revolution is considered to be the dominant effect. Due to ensemble averaging turbulence and all nonharmonic flow effects are eliminated and add only noise to the averaged period event.

If MS itself is of interest, however, class averaging has to be applied. First a trigger event is needed to identify the beginning and the end of a MS period. Here a front-wall mounted fast-response pressure transducer at ($r^* = 1.05$) was used. The signal of this sensor was measured in parallel to the signals of the fast-response probe. During MS systematic pressure fluctuations in the system (stage, pipes, cooler) can be observed. These fluctuations are typically sinusoidal. The positive-gradient zero crossing of the signal was used to determine the end of the previous and the beginning of the following MS period.

The MS frequency was 18 Hz. Therefore a reduced sampling rate of 50 kHz of the data acquisition system was chosen. The measuring time per point was set to 10.5 sec. This resulted in 196 to 197 measured MS periods per yaw position which was statistically sufficient.

The mean period length over 196 periods is very reproducible (within ±0.8‰), although individual periods may be significantly shorter or longer. Fig. 8 shows the variations during 15 consecutive data collection periods.

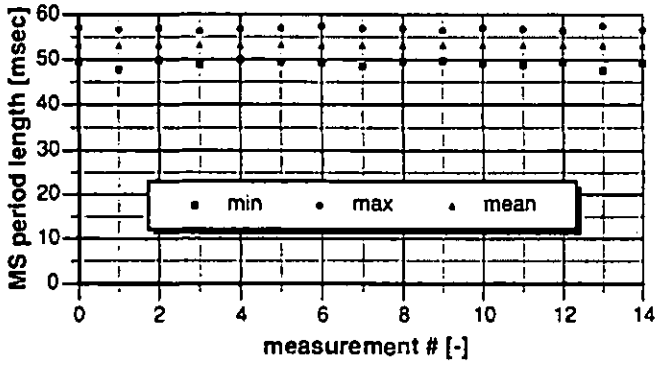

Fig. 8: Variation of the period length during MS, indicating minimum, maximum and mean lengths of MS periods

For class averaging, the signals obtained between two trigger events are subdivided into 2500 classes. Data points originating from the 196 different MS periods pertaining the same class are averaged, resulting in an ensemble averaged pressure fluctuation for one single "typical" MS period.

After class averaging the further procedure is analogous to the *pseudo-3-sensor* mode. The three measured and class averaged pressure fluctuations at each traverse position are fitted together to simulate a 3-sensor probe, giving the time-resolved flow values after performing the aerodynamic evaluation (see Part 1).

Measurement procedure during RS. The RS frequency of the stage configuration used was 42 Hz as measured by two wall pressure transducers at $r^* = 1.05$ and displaced by 44°, which showed a single cell propagating at 28% of the shaft speed. The sampling rate of the data acquisition system was set to 50 kHz. The measuring time for one position was set to 6.6 sec. resulting in 280 events (rotations of the RS cell) during each measurement.

During one RS period the flow direction is changing in a large angular domain covering up to 80°. Since the angular range (in yaw) for an accurate evaluation of 3-sensor probes is limited to 60°, an appropriate measurement procedure had to be established. In order to cover all potential flow directions in an unknown flow field the following procedure was chosen. At every traverse position the time-resolved sensor data were collected at 11 yaw positions by rotating the probe in 43° steps over one complete revolution of the probe shaft.

For data processing in a first step all measured sensor signals were class averaged. Each RS period was divided into 1000 classes. In a second step triplets of angularly neighbouring measurement positions were fitted together to simulate pseudo-*3-sensor* probes. By this procedure 9 yaw positions of a *pseudo-3-sensor* probe can be simulated per traverse position. The aerodynamic evaluation for all these probes is then performed. As a final step the probe positioned in the momentary flow direction has to be identified for each phase of the RS period. Finally the flow quantities for the whole RS can be represented by combining the flow quantities of the selected probes. This data processing mimics a 3-sensor probe which is instantaneously turned into the most appropriate yaw positions during each part of the RS period.

FLOW PHENOMENA AT STABLE OPERATING CONDITIONS

Measurements of impeller-position ensemble averaged data taken during stable operation of the stage

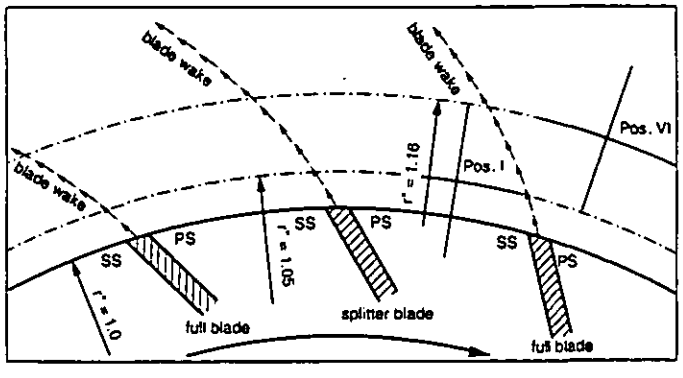

Fig. 9: Impeller blade and wake positions at the instant of triggering

Although the measurements resolved the entire perimeter, only the first three blade periods following the trigger signal will be shown. Fig. 9 shows the geometry at the instant the trigger signal is given. As seen,

a splitter-blade wake will directly arrive at Pos. I and a full-blade wake at Pos. VI. The essential features of the systematic fluctuations will be discussed by taking the nondimensional radial velocity ($C_r = c_r/u_2$) measured at Pos. I, VI, VII and IX as a reference (see Fig. 5)

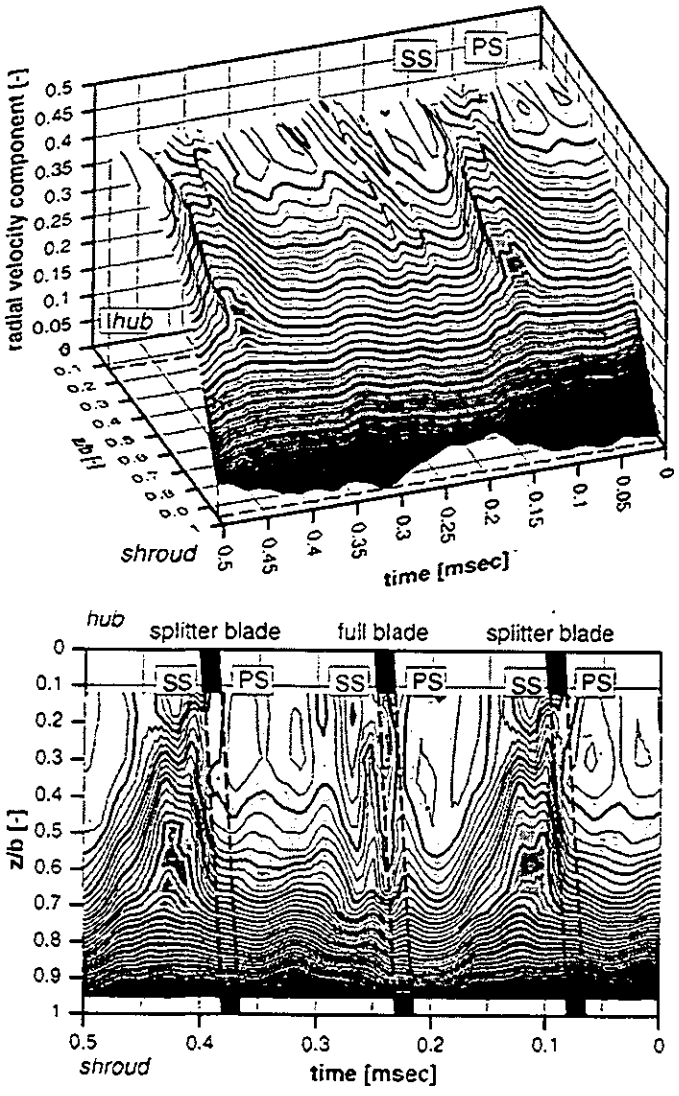

Fig. 10: Blade-resolved ensemble averaged distribution of the radial velocity component near the impeller outlet ($r^* = 1.05$, Pos. I). Running conditions: BP, Mu = 0.75. Above; 3D-view, below; top view.

Best point. In Fig. 10 - 13 the flow is plotted as it develops through the diffuser channel at a given running condition. The operating point chosen is BP with a impeller tip Mach number of Mu = 0,75 (see Tab. 1). Fig. 10 shows the flow at the impeller exit at a radius ratio $r^* = r_I/r_2 = 1.05$ in Pos. I. In the top view the impeller blade trailing edges are overlaid to the velocity plot indicating their instantaneous position projected radially to the radius 1.05. At 0.07 msec a splitter blade will pass followed by a full blade at 0.22 msec. Since the probe is located at $r^* = 1.05$ the wakes of the impeller blades arrive slightly time shifted, see Fig. 9. The time shift is a combined result of impeller blade back-lean and the spiraling character of flow in the relative frame, causing a shift corresponding to about 10% of the blade spacing at 105% radius.

The most apparent feature of the radial velocity distribution is a flow deficiency near the shroud ($z/b > 0.8$), existing even under BP conditions. This is a typical feature of open (unshrouded) impellers of the type used here. In the hub-side half of the flow annulus the C_r level is consistently high.

The second clear feature is the existence of wakes. They are parallel to the blade trailing edges and show a different topography for the full and the splitter blades. The full blade at the center of Fig. 10 shows a sharp narrow wake crossing the entire mid portion of the annulus. This *genuine blade wake* is displaced leeward (i. e., toward the suction side) by about 10% of a blade pitch, as expected in view of the back-lean of 30 degrees. Behind the splitter blades the genuine wake is weaker and can be discerned only near the hub. Another C_r deficiency is seen to occupy about half of the blade channels leeward of the splitter blades. This is the *channel wake* associated with the secondary flow distribution observed and described by ECKARDT (1975) and DEAN and SENOO (1960).

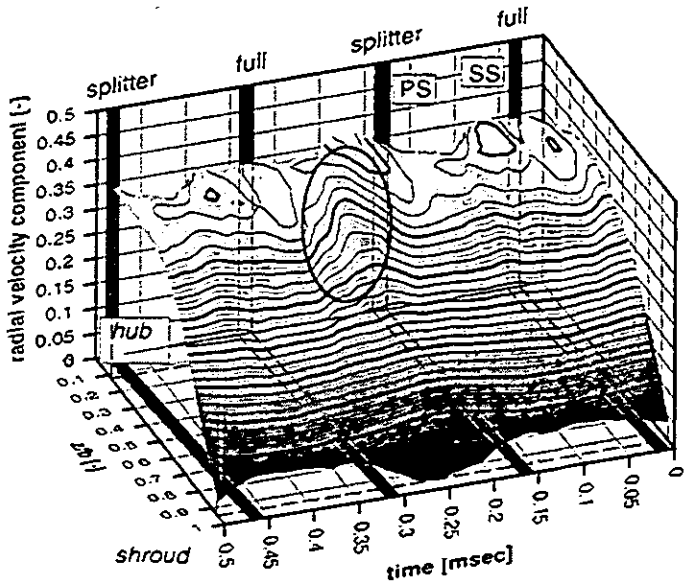

Fig. 11: As Fig. 10, (top), measured at the leading edge radius ($r^* = 1.16$, Pos. VI) of the diffuser vanes.

In Fig. 11 measurements taken at Pos. VI (see Fig. 5), the leading edge radius of the diffuser vanes ($r^* = r_{VI}/r_2 = 1.16$), are presented. The impeller blades are again overlaid to the flow distribution. Starting at 0 msec a full blade followed by a splitter blade passes the circumferential position of the probe (Pos. VI, $\vartheta = 70°$). A rough estimate shows a time delay of the flow to the blades to reach the probe of about 0.08 msec. The blade wakes are almost mixed out whereas the channel wake of the suction side of the splitter blades is still existing (encircled in Fig. 11 by an ellipse).

The characteristics of the time averaged C_r profiles from hub to shroud are seen to remain unchanged between $r^* = 1.05$ and 1.16. We can conclude: over the circumference a mixing out of the blade wakes can be observed. Every second channel wake is mixed out too. In axial direction the radial velocity distribution remains unchanged. The mean

value of the radial velocity decreases from Pos. I to Pos. VI due to the increase of the area of the flow channel according to continuity.

In Fig. 12 and Fig. 13 the radial velocity component distribution at the exit of the diffuser is plotted ($r^* = r_{VII}/r_2 = 1.70$) as measured at two circumferentially shifted probe positions, Pos. VII ($\vartheta = 77°$) and Pos. IX ($\vartheta = 83°$). A circumferentially different behavior of the radial velocity component at $r^* = 1.70$ can be seen. There is no uniform distribution at the diffuser exit, neither in the time-resolved nor in the time-mean flow distribution over the diffuser channel. Despite the totally different C_r distributions, the mass flow rate passing at Pos. VII is only 3% lower than the mass flow rate passing at Pos. IX.

The channel wakes leeward of the splitter blades are still present and can be seen at both measuring positions. During one impeller revolution 11 such wakes pass the probe. The amplitude of C_r over time at Pos. VII at $z/b = 0.5$ is roughly 4 times as big as at Pos. IX. Looking at Fig. 5 it can be seen that Pos. VII is located downstream of a diffuser blade, whereas Pos. IX is located downstream of the open diffuser channel. It is possible that at Pos. VII the flow is alternating between being part of the diffuser vane wake and the sound diffuser channel flow, resulting in high C_r fluctuations.

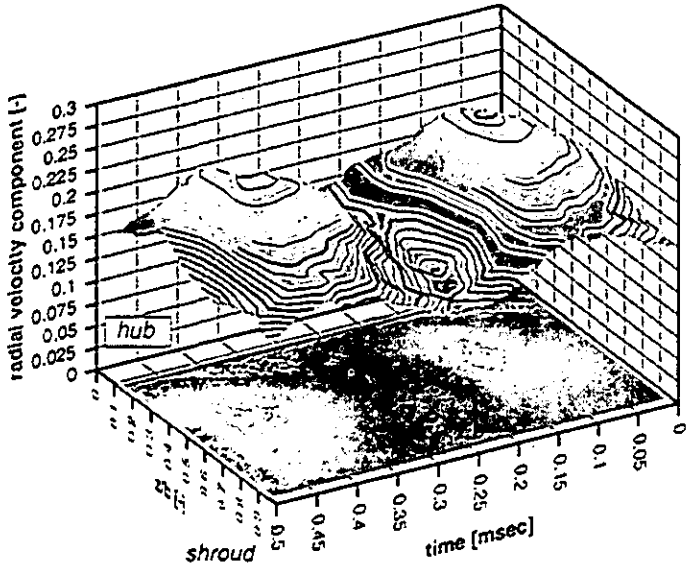

Fig. 12: As Fig. 10, (top), measured at the diffuser outlet ($r^* = 1.70$, Pos. VII).

Comparing the C_r profiles at $r^* = 1.16$ (Pos. VI, Fig. 11) and those at $r^* = 1.70$ (Pos. IX, Fig. 13) one finds a complete reversal of the hub to shroud distribution. Part of this movement in axial direction is driven by a diffuser channel vortex measured by Laser Anemometry and shown in STAHLECKER, CASARTELLI and GYARMATHY (1998).

The blade-to-blade velocity vector variations shown in Fig. 10 has been thoroughly compared to Laser-Doppler Velocimetry measurements made for the same operating conditions at the same measurements position (GIZZI, RODUNER STAHLECKER, KÖPPEL and GYARMATHY 1999), showing excellent agreement in both velocity level and flow angle.

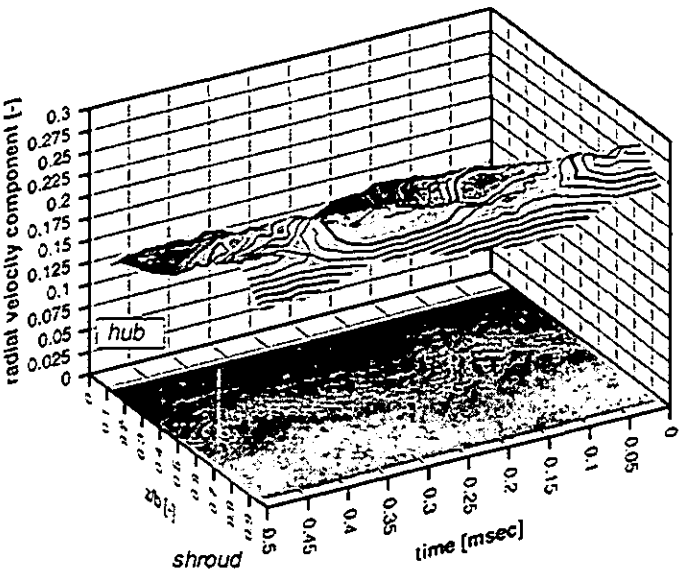

Fig. 13: Same as Fig. 12, but measured at probe Pos. IX.

Near surge. Fig. 14 shows the radial velocity component distribution at lower flow rate measured in Pos. I. The running condition for this investigations was set to "near surge" NS (see Tab. 1) with the impeller tip Mach number left unchanged at Mu = 0.75. NS is the running condition with the lowest flow rate in the stable range of operation of this centrifugal compressor.

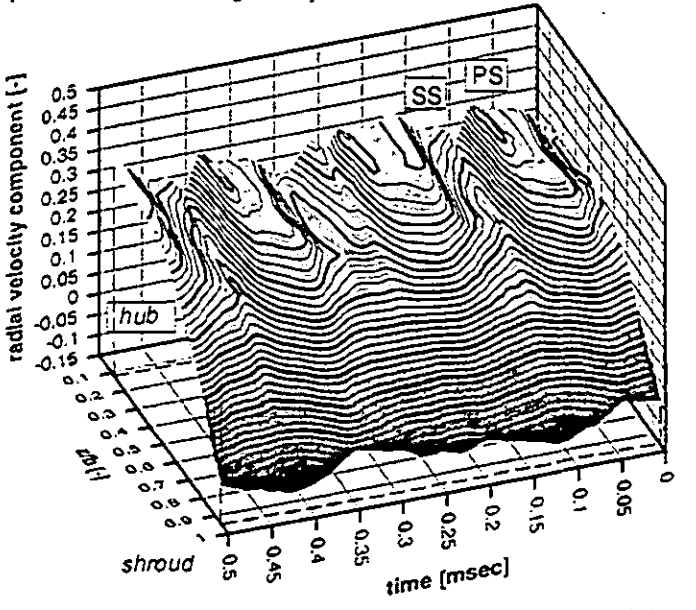

Fig. 14: Blade-resolved ensemble averaged distribution of the radial velocity component at the impeller outlet ($r^* = 1.05$, Pos. I) under steady low-flow running conditions (NS, Mu = 0.75).

Compared to the best point (Fig. 10), the C_r level has decreased and a more pronounced jet/wake flow can be observed in the impeller mid-channel hub region. The area of low radial momentum at the shroud has increased and close to the shroud a recirculation zone (negative C_r) can be observed. 10% of the diffuser channel at the impeller exit are blocked

due to this recirculation.

FLOW PHENOMENA AT UNSTABLE OPERATING CONDITIONS

Measurements of impeller position ensemble averaged data taken during unstable operation of the stage

For the measurements plotted in Fig. 15 the flow rate was set to MS (see Tab. 1). The tip speed Mach number was again Mu = 0.75. MS is a running condition in the unstable regime of the performance map. During MS pressure fluctuations of the whole piping system at 18 Hz are present resulting in fluctuating flow rate and pressure rise of the stage. In Fig. 15 the ensemble averaged radial velocity distribution over the channel position and time is plotted. For ensemble averaging, the once per revolution signal of the impeller shaft trigger was used. Since impeller rotation and MS are nonharmonic phenomena the pressure fluctuations of MS are statistically mixed out in this plot and contribute only to the pressure fluctuation level. The character of the C_r distribution remains unchanged compared to NS075. According to the lower flow rate at MS the C_r mean value is slightly lower.

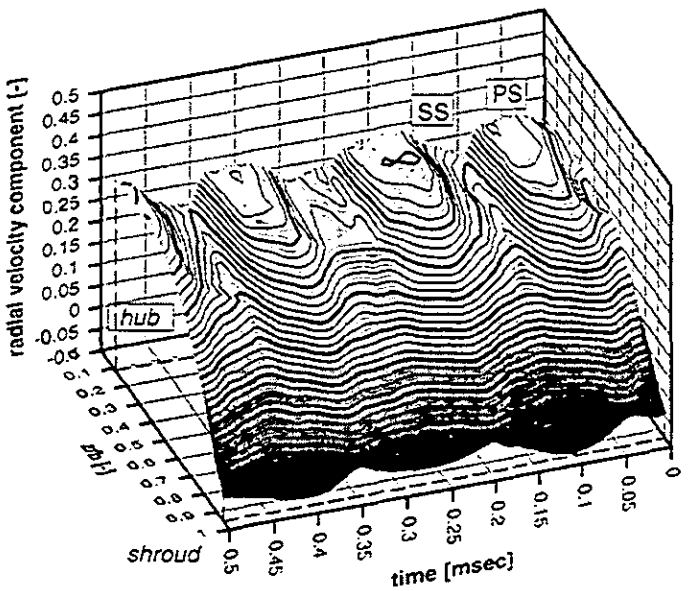

Fig. 15: Blade-resolved ensemble averaged distribution of the radial velocity component at the impeller outlet (r* = 1.05, Pos. I) during mild surge (MS, Mu = 0.75).

Measurements of class averaged data during unstable running conditions of the stage

Measurements during MS. In order to investigate the systematic fluctuations due to mild surge the above described class averaging procedure was applied to the data yielding in Fig. 15. The results are shown in Fig. 16 and 17.

Looking at the performance map (Fig. 7) the range of stable operating points is separated from the unstable range of operation by the vertex of the speedlines. To the right (negative gradients) the compressor operates stable. On the side of the positive gradients the compressor operates in the unstable range. Here small perturbations of

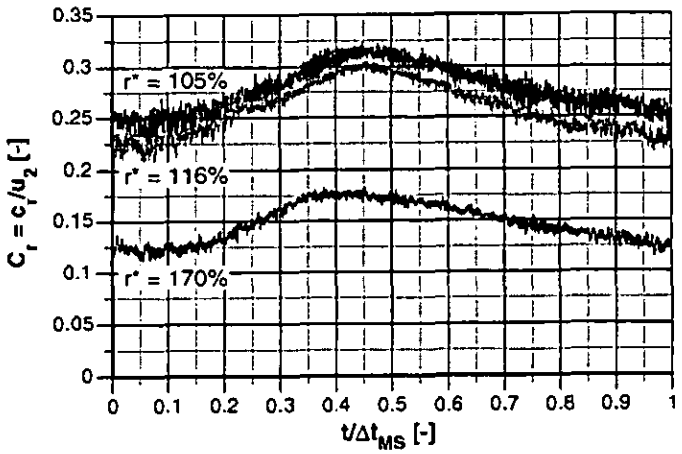

Fig. 16: Class averaged C_r variation at mid-channel, measured at three different diffuser positions plotted over one MS period (MS, Mu = 0.75, z/b = 0.48).

the flow rate lead to an input of energy into the dynamic flow system resulting in periodic pressure and flow rate fluctuations. For detailed information see RIBI (1997) and GREITZER (1981).

The C_r data presented in Fig. 16 were taken at mid-channel at three different position of the diffuser, at Pos. I (r* = 1.05), at Pos. VI (r* = 1.16) and at Pos. IX (r* = 1.70). Plotted are class averaged results for a single MS period. For each MS period about 16 impeller rotations occur according to the MS frequency of 18 Hz.

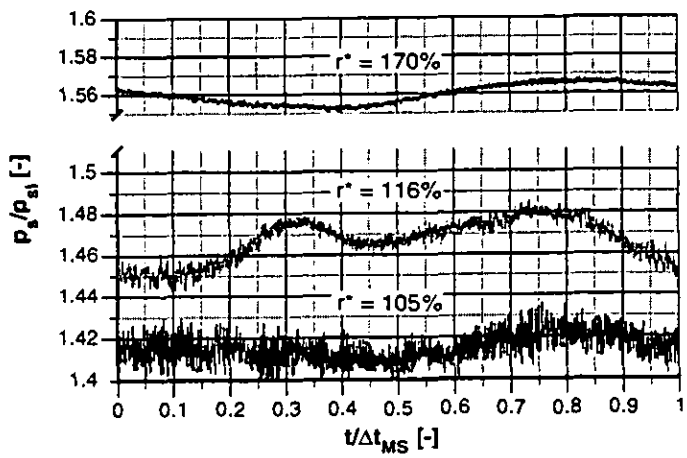

Fig. 17: Class averaged static pressure variation during mild surge at mid-channel, measured at three different diffuser positions, plotted over one MS period (MS, Mu = 0.75, z/b = 0.48).

The C_r distributions in Fig. 16 show an approximately harmonic variation of the mass flow during an MS period. Downstream of the diffuser the amplitude of the C_r fluctuations is smaller due the lower velocity level. Fig. 17 shows the static pressure fluctuations during mild surge. While a sinusoidal variation is seen at diffuser exit (r* = 1.70), at the throat (r* = 1.16) higher harmonics occur. A discussion of these unsteady phenomena is beyond the scope of the present paper.

Measurements during RS. Since persistent operation in rotating stall cannot be achieved in the present compressor at Mu = 0.75, the measurements were performed at Mu = 0.4 where RS occurs as a stable phenomenon. At the measured running conditions (RS04, see Tab. 1) and the present stage configuration single cell full span rotating stall is observed.

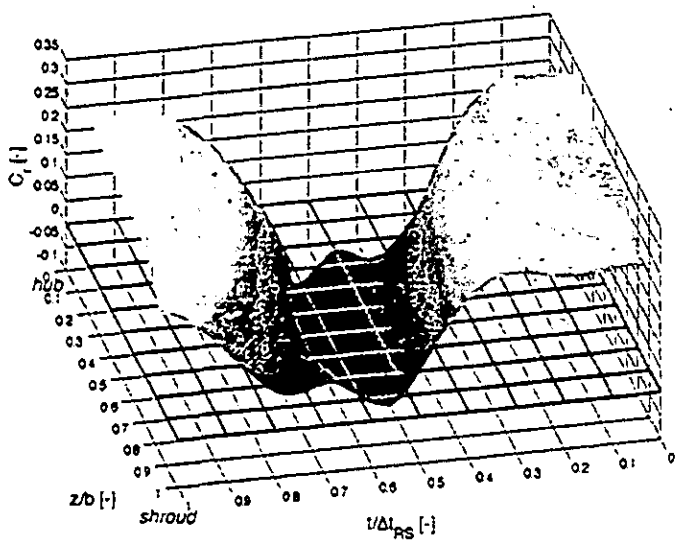

Fig. 18: Class averaged C_r distribution measured at the impeller exit during rotating stall (Pos. I, r* = 1.05) plotted over one RS period (RS, Mu = 0.4).

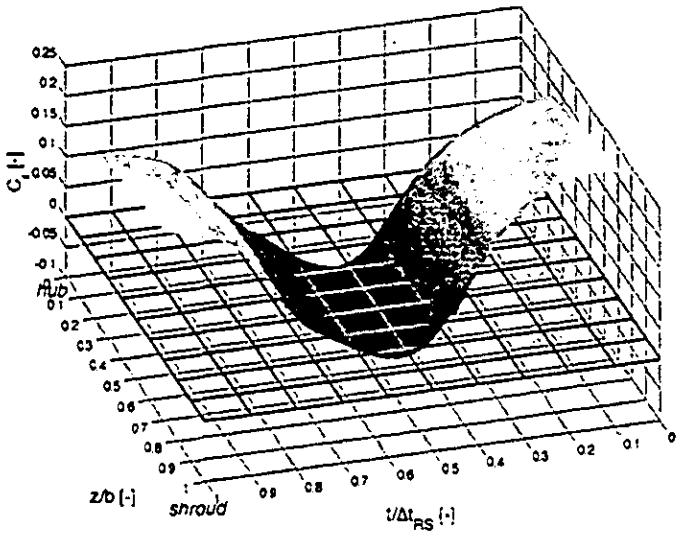

Fig. 19: As Fig. 18, but measured at the diffuser exit (Pos. IX, r* = 1.70).

In Fig. 18 to 21 class averaged data are presented. In order to show that during RS the entire channel is temporarily blocked, in Fig. 18 the C_r distribution from hub to shroud is plotted. The data presented in Fig. 18 were measured at the impeller exit (Pos. I). Fig. 19 shows the same distribution measured at the diffuser exit at Pos. IX. At the impeller exit as well as at the diffuser exit a zone of blocked or reverse flow covering about 25% of the diffuser area can be observed. The phenomenon is seen to be very nearly two dimensional. The stall cell propagates around the circumference at about 28% of the impeller speed (RIBI 1993, GYARMATHY 1996)

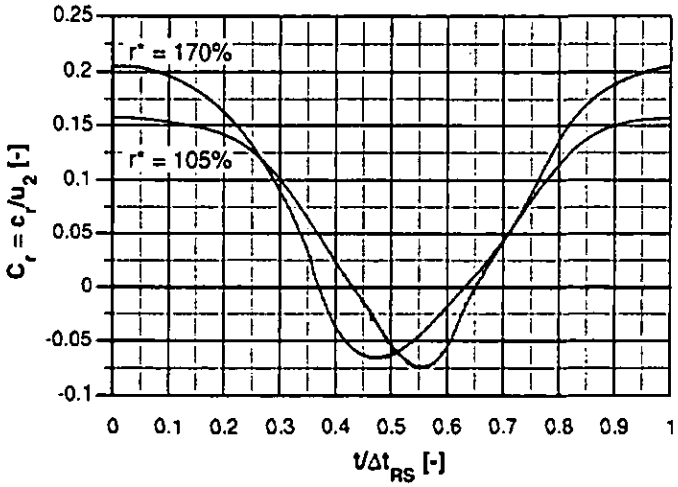

Fig. 20: Class averaged C_r variation during rotating stall, measured at mid-channel at diffuser inlet and outlet, plotted over one RS period (RS, Mu = 0.4, z/b = 0.48).

Fig. 20 shows the mid-channel radial velocity component fluctuation during one RS period at the inlet and outlet of the diffuser (probe positions I and IX, r* = 1.05 and 1.70). The impeller rotates approximately 3 times during one revolution of the RS cell. This results in roughly 70 impeller blade passages during one RS period. In order to check the mass continuity condition, the area weighted integrals of c_r measured at the diffuser inlet and the diffuser outlet at mid channel (z/b = 0.48), over one entire RS period were compared:

$$1{,}05 \int_0^{\Delta t_{RS}} c_{r105}\, dt = 1{,}70 \int_0^{\Delta t_{RS}} c_{r170}\, dt \qquad (1)$$

The difference between the two integrals was found to be only 0.6%. This good agreement in terms of the continuity is reassuring, although a conclusive check would require an integration of hub to shroud instead of using the mid-channel c_r values.

Another aspect of the curves seen in Fig. 20 is a time shift in the passage of the cell. Both the beginning and the end of reverse flow is registered *earlier* at the exit of the diffuser than at the inlet, the time shift being 0.06 units for the front and 0.02 units for the rear edge of the cell. As seen in Fig. 5, the probe at Pos. IX is exposed to flow coming from the diffuser channel *preceding* the channel pertaining to Position I. Therefore an earlier probe response to channel blockage events is expected at diffuser exit, the shift being 1/24 = 0.042. This corresponds well to the shift measured and is another confirmation of mass continuity.

The total and static pressure fluctuations at Pos. I and IX, class averaged over one RS period are shown in Fig. 21. While the recirculating zone passes the probe the difference between total and

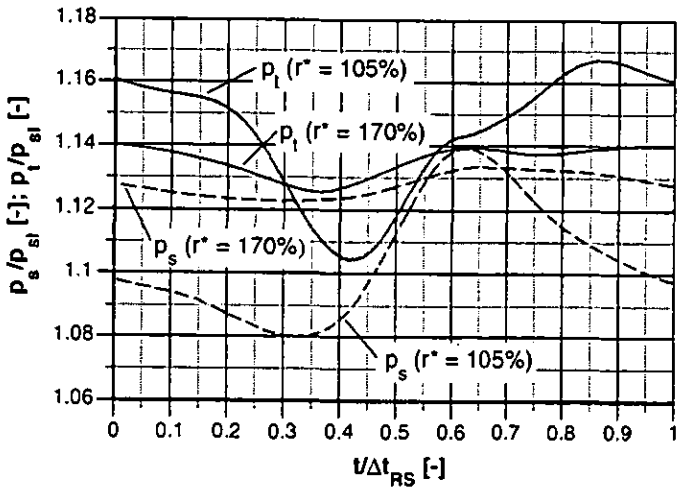

Fig. 21: Same as Fig. 20, showing the class averaged total and static pressure variations.

static pressure is very small due to the very small velocities present in the stall cell.

Seen from the absolute (nonrotating) frame of the probe located at Pos. I ($r^* = 1.05$), the following phenomena during one RS period starting at $t/\Delta t_{RS} = 0$ can be observed. The passage of one RS period, one circumferential rotation of a RS cell, can be divided into four sections.

- Section 1 ($t/\Delta t_{RS}$ = 0 - 0.2); the sound flow of non-blocked impeller channels with positive C_r values passes the probe.
- Section 2 ($t/\Delta t_{RS}$ = 0.2 - 0.4); the velocity drops and the flow angle α_2 decreases. Total and static pressure decrease and approach each other.
- Section 3 ($t/\Delta t_{RS}$ = 0.4 - 0.65): now the probe is downstream of the blocked impeller channels. C_r is low and negative. Dynamic head is small due to the small velocities. The static pressure is increasing.
- Section 4 ($t/\Delta t_{RS}$ = 0.65 - 1.0): The stagnant fluid is blown away by sound throughflow coming form the impeller. Velocity and α_2 increase. Due to the acceleration of the flow the static pressure decreases.

In GYARMATHY (1996) RS is described as impeller-diffuser momentum exchange. This model is in good agreement to the measured pressure traces during one RS period. Stopping and reversing the forward flow is associated with a static pressure minimum in the impeller/diffuser interspace, while its re-start requires a pressure maximum. The edges of the cell ($C_r = 0$) closely coincide with the static pressure peaks. The pressure amplitudes are small downstream of the diffuser.

SUMMARY AND CONCLUSIONS

The FRAP® System involving a 1-sensor probe as described in Part 1 of these contributions has been applied to several types of systematic flow fluctuations occurring in the stable and unstable range of operation of a centrifugal compressor. The time-resolved data were analysed and interpreted to reveal detailed features of the processes involved.

System applicability

The probes proved to be rugged and reliable instruments giving accurate high-resolution data in a narrow (16.8 mm) diffuser channel at high shaft speeds with blade passing frequencies of typically 6.5 kHz. Normally, the sampling rate was set to 200 kHz.

A wall-to-wall traverse typically comprised 13 measuring positions with the data collecting time totalling 2.5 seconds per position (0.82 sec each in three yaw angle positions), permitting statistical averaging over 242 rotor resolutions for sake of suppressing turbulence effects.

Higher collection times (10.5 sec) in each of the three yaw positions were requested during mild surge where the averaging was based on about 200 surge cycles of low-frequency (18 Hz), and the sampling rate was reduced to 50 kHz.

During rotating stall (42 Hz) the measurements had to include periods of back flow. Therefore the number of yaw positions has been increased to eleven, leading to data collection times of 6.6 x 11 = 72.6 seconds (at 50 Hz sampling rate) per traverse position. This yielded an ample statistical basis including 280 cell rotations.

The statistically reliable and coherent (pseudo-simultaneous) measurement of velocity vector and pressure data opens up new avenues for the interpretation of unsteady flow phenomena. An example is the phase relationship between pressure and velocity fluctuations during stall and surge processes.

Flow phenomena observed

In the ***stable range*** measurements performed at different diffuser positions for two operating points at the same shaft speed (BP075 and NS075) have lead to following conclusions with respect to the stage investigated.

- The impeller *blade wakes* mix out in the vaneless region perceding the diffuser.
- Impeller *channel wakes*, originating from the "jet/wake" distribution, located near the suction side of the splitter blades are capable of propagating through the vaned diffuser and can still be measured at the diffuser exit while the wakes located at the suction side of the full blades are mixed out. Therefore half of the impeller blade passing frequency is found to be predominant at the diffuser exit.
- The shroud-side *circumferential zone* of low radial momentum existing all around the impeller exit is mixed out as the flow passes through the diffuser.

Measurements performed in the unstable range of operation during ***mild surge*** have shown that the blade-to-blade radial velocity distributions fluctuate in level but maintain their character in time.

Measurements performed in the unstable range of operation during ***rotating stall*** have shown that

- single cell full span RS occurs
- the measurements are in good agreement with the description of RS as a momentum exchange phenomenon proposed in GYARMATHY (1996).

It can be concluded: Even a 1-sensor fast-response probe is a very valuable tool for investigating time-dependent systematic flow phenomena occurring in turbomachines. A highly detailed insight into blade passing, mild surge or rotating stall can be achieved not only

qualitatively but quantitatively with high accuracy and resolution.

ACKNOWLEDGMENTS

The authors would like to thank the Swiss Commission for Technology and Innovation (CTI), ABB Turbo Systems Ltd and Sulzer Turbo Ltd for their financial support. They also wish to thank all the technical staff of the laboratory for their support.

REFERENCE

Bammert, K., and Rautenberg, M., 1974, „On the Energy Transfer in Centrifugal Compressors", *ASME-Paper 74-GT-121.*

Dean, R. C. Jr., and Senoo, Y., 1960, „Rotating Wakes in Vaneless Diffusers", *Journal of Basic Engineering,* September 1960.

Dean, R. C. Jr., and Young, L. R., 1977, „The Time Domain of Centrifugal Compressor and Pump Stability and Surge", *Journal of Fluids Engineering,* March 1977.

DIN 1952, 1982, „Durchflussmessung mit Blenden, Düsen und Venturirohren in voll durchströmten Rohren mit Kresisquerschnitt" Beuth Verlag GmbH, Berlin, Germany.

Eckardt, D., 1975, „Instantaneous Measurements in the Jet-Wake Discharge Flow of a Centrifugal Compressor Impeller", *Journal of Engineering for Power,* July 1975.

Eckardt, D., 1976, „Detailed Flow Investigations Within a High-Speed Centrifugal Compressor Impeller", *Journal of Fluids Engineering,* September 1976.

Gizzi, W., Roduner, C., Stahlecker, D., Köppel, P., and Gyarmathy, G., 1999, „Time Resolved Measurements with Fast-Response Probes and Laser-Doppler-Velocimetry at the Impeller Exit of a Centrifugal Compressor - A Comparison of Two Measurements Techniques", *3rd European Conference on Turbomachinery,* London 1999.

Greitzer, E. M., 1981, „The Stability of Pumping Systems", *Journal of Fluids Engineering,* Vol. 103.

Gyarmathy, G., 1996, „Impeller-Diffuser Momentum Exchange During Rotating Stall", *ASME Paper 96-WA/PID-6.*

Hathaway, M. D., Chriss, R. M., Wood, J. R., and Strazisar, A. J., 1993, „Experimental and Computational Investigation of the NASA Low-Speed Centrifugal Compressor Flow Field", *Journal of Turbomachinery,* July 1993.

Hunziker, R., 1993, „Einfluss der Diffusorgeometrie auf die Instabilitätsgrenze des Radialverdichters", *PhD-thesis No. 10252,* ETH Zürich, Switzerland.

Hunziker, R., and Gyarmathy, G., 1993, „The Operational Stability of a Centrifugal Compressor and its Dependence on the Characteristics of the Subcomponents", *ASME-Paper 93-GT-284.*

Kämmer, N., and Rautenberg, M., 1982, "An Experimental Investigation of Rotating Stall Flow in a Centrifugal Compressor", *ASME Paper 82-GT-82.*

Krain, H., 1981, "A Study on Centrifugal Impeller and Diffuser Flow", *Journal of Engineering for Power,* October 1981, Vol. 103.

Jansen, W., 1964, „Rotating stall in a Radial Vaneless Diffuser", *Journal of Basic Engineering,* December 1964.

Inoue, M., and Cumpsty, N. A., 1984, „Experimental Study of Centrifugal Impeller Discharge Flow in Vaneless and Vaned Diffusers", *Journal of Engineering for Gas Turbines and Power,* April 1984.

Kämmer, N., and Rautenberg, M., 1982, „An Experimental Investigation of Rotating Stall Flow in a Centrifugal Compressor", *ASME Paper 82-GT-82.*

Kupferschmied, P., 1998, „Zur Methodik zeitaufgelöster Messungen mit Strömungssonden in Verdichter und Turbinen", *Dissertation ETH Nr. 12774,* ETH Zürich, Switzerland.

Ng, W. F., and Epstein, A. H., 1985, „Unsteady Losses in Transonic Compressors", *Journal of Engineering for Gas Turbines and Power,* April 1985.

Ribi, B., and Gyarmathy, G., 1993, „Impeller Rotating Stall as a Trigger for the Transition from Mild Surge to Deep Surge in a Subsonic Centrifugal Compressor", *ASME-Paper 93-GT-234.*

Ribi, B., 1996, „Radialverdichter im Instabilitätsbereich", *Dissertation ETH Nr. 11717,* ETH Zürich, Switzerland.

Ribi, B., 1997, „Energy Input of a Centrifugal Stage Into the Attached Piping System During Mild Surge", *ASME Paper 97-GT-84.*

Roduner, C., Köppel, P., Kupferschmied, P., and Gyarmathy, G., 1998, „Comparison of Measurement Data at the Impeller Exit of a Centrifugal Compressor Measured with both Pneumatic and Fast-Response Probes", *ASME Paper 98-GT-241.*

Runstadler, P. W. Jr., and Dolan, F. X., 1975, "Design, Development, and Test of a Laser Velocimeter for High Speed Turbomachinery", *Proceedings of the LDA-Symposium,* Copenhagen 1975.

Stahlecker, D., and Gyarmathy, G., 1998, „Investigations of Turbulent Flow in a Centrifugal Compressor Vaned Diffuser by 3-Component Laser Velocimetry", *ASME Paper 98-GT-300.*

Stahlecker, D., Casanelli, E., and Gyarmathy, G., 1998, „Secondary Flow Field Measurements With a LDV in the Vaned Diffuser of a High-Subsonic Centrifugal Compressor", *9th International Symposium on Application of Laser Techniques to Fluid Mechanics,* Lissabon 1998.

Traupel, W., 1988, „Thermische Turbomaschinen I", Springer-Verlag, Berlin, p. 307.

Walbaum, M., and Riess, W., 1998, „Einfluss der Leitschaufelverstellung auf die Entwicklungsformen des Rotating Stall in mehrstufigen Verdichtern", *VDI Berichte 1425.*